# Advanced Models for the Static and Dynamic Analyzes of Wing and Fuselage Structures

M. Filippi*, A. Pagani†,
E. Carrera‡, M. Petrolo§ and E. Zappino¶
*Politecnico di Torino, Corso Duca degli Abruzzi 24, 10129 Torino, Italy.*

**This paper proposes advanced 1D theories for the static and dynamic analyzes of aeronautical structures. Hierarchical formulation was introduced by adopting polynomial expansions of the displacement field above the structure cross-section. Two classes of 1D higher-order models were developed according to the Carrera Unified Formulation (CUF). Lagrange Expansion (LE) models were built by means of four- (L4) and nine-point (L9) Lagrange-type polynomials. Instead, Taylor Expansion (TE) models exploit N-order Taylor-like polynomials. Classical models may be obtained as special cases of TE. The finite element method was exploited to develop numerical applications by employing the principle of virtual displacements. In the CUF framework the finite element matrices and vectors are expressed in terms of fundamental nuclei whose forms do not formally depend on the order and the class of the model. A number of typical stiffened-shell structures were analyzed. Classical 1D (Euler-Bernoulli and Timoshenko) and refined models were implemented by exploiting the 1D CUF. Finite element models by a commercial software were used for comparison purposes. Results have highlighted the enhanced capabilities of the present formulation which is able to detect solid and shell-like accuracies with significantly lower computational costs.**

## Nomenclature

| | |
|---|---|
| $\boldsymbol{C}$ | Material stiffness matrix |
| $\boldsymbol{D}$ | Linear differential operator matrix |
| $\mathbf{q}_{\tau i}$ | Nodal displacement vector |
| $\mathbf{u}$ | Displacement vector |
| $\mathbf{u}_\tau$ | Generalized displacement vector |
| $F_\tau$ | Cross-section function |
| $L_{ext}$ | External work |
| $L_{ine}$ | Work of the inertial loadings |
| $L_{int}$ | Internal work |
| $N$ | Order of the expansion above the cross-section for the TE models |
| $N_i$ | Shape function |
| $u_x$, $u_y$, $u_z$ | Displacement components in the $x$, $y$ and $z$ directions |
| $x$, $y$, $z$ | Coordinates reference system |

*Symbols*

| | |
|---|---|
| $\boldsymbol{\epsilon}$ | Strain vector |
| $\boldsymbol{\sigma}$ | Stress vector |
| $\delta$ | Virtual variation |

*Ph.D. Student, Department of Mechanical and Aerospace Engineering, matteo.filippi@polito.it
†Ph.D. Student, Department of Mechanical and Aerospace Engineering, alfonso.pagani@polito.it
‡Professor, Department of Mechanical and Aerospace Engineering, erasmo.carrera@polito.it, AIAA Member
§Research Assistant, Department of Mechanical and Aerospace Engineering, marco.petrolo@polito.it
¶Ph.D. Student, Department of Mechanical and Aerospace Engineering, enrico.zappino@polito.it

# I. Introduction

AIRCRAFT structures are essentially reinforced thin shells. The so-called *semimonocoque* constructions are composed by three main components: skins (or panels), longitudinal stiffening members and transversal members. Skins have the function to transmit aerodynamic forces and to act with the longitudinal members in resisting the applied loads. Stringers resist bending and axial loads above the skin. Finally, ribs are mainly used to maintain the cross-sectional shape and to redistribute concentrated loads into the structure.

Wings and fuselages are subject to many different types of mechanical and aerodynamics loads throughout their operational life. These loads give rise to vibration in structures leading to structural fatigue, flutter and noise transmission. Many different approaches were developed in the first half of the last century for the determination of stress/strain fields in these structural components. These approaches are discussed in major reference books.[1,2]

In the classical Finite Element Method (FEM) framework, reinforced-shell structures are generally described as complex systems in which one-dimensional (rod/beam) and two-dimensional (plate/shell) structural elements are properly assembled. A number of works have shown the necessity of a proper simulation of the stiffeners-panel "linkage".[3,4,5] 3D finite element models are usually implemented as soon as the wing's structural layouts are determined. Because of their complexity, solid models are commonly used only within optimization procedures. In fact, despite the availabilities of even more cheaper computer power, these FEM models present large computational costs.

The present paper proposes a new approach in the analysis of complex aircraft structures. Higher order one-dimensional models, based on the Carrera Unified Formulation (CUF), are used. Several refined beam models have been developed to overcome the limitations of the classical beam theories by Euler-Bernoulli (EBBT) and Thimoshenko (TBT). The first attempts dealt with the introduction of shear correction factors, such as in Ref. 6. Works by Dinis, Camotim and Silvestre[7] and Silvestre[8] dealt with the buckling analysis of thin walled open/closed cross-section beams: the Generalized Beam Theory (GBT) was used to implement beam theories accounting for the in-plane cross-section deformations, and shell-type results were obtained by using appropriate cross-section shape functions describing the beam displacement field; the choice of those functions depends on the geometry of the considered structures.

CUF 1D models have been recently developed[9] and are based on a hierarchical formulation which considers the order of the theory as an input of the analysis. Two classes of CUF 1D models have been proposed: the Taylor-expansion class, hereafter referred to as TE, and the Lagrange-expansion class, hereafter referred to as LE. The finite element formulation was adopted to deal with arbitrary geometries, boundary conditions and loadings.

A number of significant problems dealing with reinforced-shell structures are addressed in the following. The paper is organized as follows: a brief description of the CUF is given in Section II; numerical results are provided in Section III; main conclusions are then outlined in Section IV.

# II. Refined 1D Models

A brief overview on the theoretical model is herein provided. The adopted coordinate frame is presented in Fig. 1.

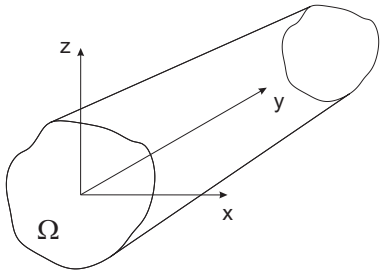


**Figure 1. Coordinate frame of the beam model.**

The transposed displacement vector is defined as

$$\mathbf{u}(x,y,z;t) = \left\{ \begin{array}{ccc} u_x & u_y & u_z \end{array} \right\}^T \tag{1}$$

Stress, $\boldsymbol{\sigma}$, and strain, $\boldsymbol{\epsilon}$, components are

$$\boldsymbol{\sigma} = \left\{ \begin{array}{cccccc} \sigma_{xx} & \sigma_{yy} & \sigma_{zz} & \sigma_{xy} & \sigma_{xz} & \sigma_{yz} \end{array} \right\}^T, \quad \boldsymbol{\epsilon} = \left\{ \begin{array}{cccccc} \epsilon_{xx} & \epsilon_{yy} & \epsilon_{zz} & \epsilon_{xy} & \epsilon_{xz} & \epsilon_{yz} \end{array} \right\}^T \tag{2}$$

Linear strain-displacement relations were used,

$$\boldsymbol{\epsilon} = \boldsymbol{D}\mathbf{u} \tag{3}$$

where $\boldsymbol{D}$ is a linear differential operator whose explicit expression is not reported here for the sake of brevity, it can be found in Ref. 9.
Constitutive laws were exploited to obtain stress components,

$$\boldsymbol{\sigma} = \boldsymbol{C}\boldsymbol{\epsilon} \tag{4}$$

The components of $\boldsymbol{C}$ are the material coefficients. They can be found in Reddy's book.[10]

### II.A. Unified Formulation

In the CUF framework, the displacement field is the expansion of generic functions, $F_\tau$:

$$\mathbf{u} = F_\tau \mathbf{u}_\tau, \qquad \tau = 1, 2, ...., M \tag{5}$$

where $F_\tau$ vary above the cross-section. $\mathbf{u}_\tau$ is the generalized displacement vector and $M$ stands for the number of terms of the expansion. According to the Einstein notation, the repeated subscript, $\tau$, indicates summation. The choice of $F_\tau$ determines the class of 1D CUF model to adopt.

The Taylor Expansion class (TE) is based on $N$-order Taylor-like polynomial expansions, $x^i\, z^j$, of the displacement field above the cross-section of the structure ($i$ and $j$ are positive integers). The order $N$ of the expansion is arbitrary and is set as an input of the analysis. Static[11,12] and free-vibration analyzes[13,14] showed the strength of CUF 1D models in dealing with arbitrary geometries, thin-walled structures and local effects. Moreover, asymptotic-like analyzes leading to reduced refined models were carried out in Ref. 15. The Euler-Bernoulli (EBBT) and Timoshenko (TBT) classical beam theories were derived from the linear ($N = 1$) Taylor-type expansion.

The Lagrange Expansion class (LE) exploits Lagrange polynomials to build 1D refined models. Different types of cross-section polynomial sets can be adopted: nine-point elements, L9, four-point elements, L4, etc. LE models have only pure displacement variables. Static analyzes on isotropic[16] and composite structures[17] revealed the strength of LE models in dealing with open cross-sections, arbitrary boundary conditions and obtaining Layer-Wise descriptions of the 1D model.

Classical, refined and *component-wise* (CW) models can be implemented by means of CUF 1D. "Component-wise" means that each typical component of a reinforced-shell structure (i.e. stringers, sheet panels and ribs) can be modeled by means of a unique 1D formulation and, therefore, with no need of *ad hoc* formulations for each component. This methodology permits us to tune the model capabilities by 1. choosing which component requires a more detailed model; 2. setting the order of the structural model to be used. For more details about CW models see Ref. 18, 19.

### II.B. Finite Element Formulation

The FE approach was adopted to discretize the structure along the $y$-axis. This process is conducted via a classical finite element technique, where the displacement vector is given by

$$\mathbf{u}(x, y, z; t) = F_\tau(x, z) N_i(y) \mathbf{q}_{\tau i}(t) \tag{6}$$

$N_i$ stands for the shape functions and $\mathbf{q}_{\tau i}$ for the nodal displacement vector,

$$\mathbf{q}_{\tau i} = \left\{ \begin{array}{ccc} q_{u_{x_{\tau i}}} & q_{u_{y_{\tau i}}} & q_{u_{z_{\tau i}}} \end{array} \right\}^T \tag{7}$$

The explicit forms of the shape functions $N_i$, are not reported here, they can be found in the book by Bathe.[20]

The stiffness and mass matrices of the elements, and the external loadings that are coherent to the models were obtained via the Principle of Virtual Displacements:

$$\delta L_{int} = \delta L_{ext} - \delta L_{ine} \tag{8}$$

where $L_{int}$ stands for the strain energy, $L_{ext}$ is the work of the external loadings, and $L_{ine}$ is the work of the inertial loadings. $\delta$ stands for the virtual variation. $L_{int}$, $L_{ext}$, and $L_{ine}$ can be written as follows:

$$\delta L_{int} = \delta \mathbf{q}_{\tau i}^T \mathbf{K}^{ij\tau s} \mathbf{q}_{sj}, \qquad \delta L_{ext} = F_\tau N_i \mathbf{P} \delta \mathbf{q}_{\tau i}^T, \qquad \delta L_{ine} = \delta \mathbf{q}_{\tau i}^T \mathbf{M}^{ij\tau s} \ddot{\mathbf{q}}_{sj} \tag{9}$$

where $\mathbf{K}^{ij\tau s}$ and $\mathbf{M}^{ij\tau s}$ are the fundamental nuclei of the stiffness matrix and the mass matrix, respectively. $\mathbf{P}$ is a generic concentrated load. The nucleus components of $\mathbf{K}$ and $\mathbf{M}$ do not formally depend on the approximation order. This is the key-point of the CUF which allows us, with only nine FORTRAN statements, to implement any-order beam theories. The derivation of the fundamental nuclei is not reported here for the sake of brevity, but it is given in previous works by Carrera and his co-workers,[9,21] together with a more detailed overview on the CUF.

## III. Numerical Results

Static and free vibration analyzes of typical aeronautical structures were performed and the results by 1D CUF models were compared to the results from MSC/NASTRAN©. In the first part of this section the static analysis of a three-bay wing box is presented. The carried out study allows us to show the capability of the present refined 1D models of dealing with ribs and open sections. In the second part of this section the modal analysis of a fuselage structure is considered. The attention is focused on the capability of the present models of dealing with solid and shell-like FEM analyzes as well as with very low computational costs. Further results about wing and fuselage structures analyzes can be found in Ref. 18, 19, 22.

### III.A. Static Analysis of a Three-bay Wing Box

A static analysis of the wing structure presented in Fig. 2a was carried out. This structure consists of a three-bay box beam having a trapezoidal cross-section. The stringers are considered rectangular for convenience, however their shape does not effect the validity of the proposed analysis. Figures 2b and 2c show the geometrical configurations of the multi-bay wing with no ribs and with the open mid-bay cross-section, respectively. These examples allow us to highlight the capability of the present advanced 1D models to accurately describe the effects due to ribs and open sections.

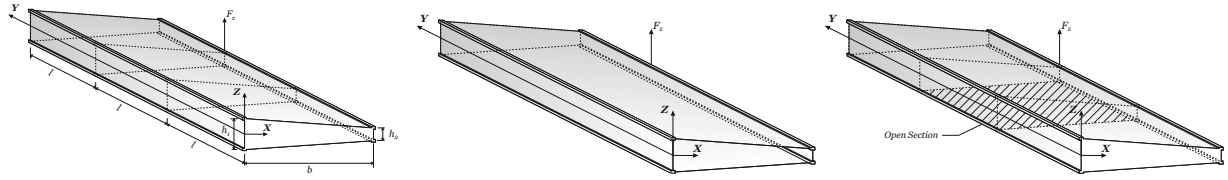


(a) Full model (b) No ribs case (c) Full model with the open mid-bay

**Figure 2. The different structural configurations of the three-bay wing box.**

Each bay presents a length, $l$, equal to 0.5 $[m]$. The cross-section is a trapezium having height $b = 1$ $[m]$. The two spars webs have a thickness of $1.6 \times 10^{-3}$ $[m]$, whereas $h_1 = 0.16$ $[m]$ and $h_2 = 0.08$ $[m]$. The top and the bottom panels have a thickness of $0.8 \times 10^{-3}$ $[m]$, as well as ribs. The stringers area is $A_s = 8 \times 10^{-4}$ $[m^2]$. The wing is completely made of an aluminium alloy 2024, having $G/E = 0.4$. The cross-section in $y = 0$ is clamped, whereas a point load, $F_z = 2 \times 10^4$ $[N]$, is applied at $[b, 2 \times l, h_2/2]$.

Table 1 shows vertical displacement values, $u_z$ and the number of the degrees of freedom for each model. Results related to CUF models were validated by an MSC/NASTRAN© model built both with solid and shell FE elements (both stringers and ribs were discretized by means of solid elements, whereas shell elements were used for skins and webs). The increasing order Taylor-type models are considered in rows $4^{th}$ to $7^{th}$. $N$ refers to the expansion order of the TE model. The LE model was implemented by discretizing the cross-section of each component as follows: stringers and panels/webs are composed by 1 L9 element each; the ribs are discretized with a combination of L4 and L9 elements.

**Table 1. Displacement values, $u_z$, at loaded point and number of degrees of freedom for the three-bay wing box.**

| | Case 1, fig. 2a | | Case 2, fig. 2b | | Case 3, fig. 2c | |
|---|---|---|---|---|---|---|
| | $u_z \times 10^2$ [m] | DOFs | $u_z \times 10^2$ [m] | DOFs | $u_z \times 10^2$ [m] | DOFs |
| | | | MSC/NASTRAN© | | | |
| | 1.412 | 100026 | 3.051 | 89400 | 1.963 | 89621 |
| | | | Classical Beam Theories | | | |
| EBBT | 0.464 | 495 | 0.464 | 495 | 0.464 | 495 |
| TBT | 0.477 | 495 | 0.477 | 495 | 0.477 | 495 |
| | | | TE | | | |
| $N = 3$ | 0.793 | 1650 | 0.794 | 1650 | 0.873 | 1650 |
| $N = 5$ | 1.108 | 3465 | 1.203 | 3465 | 1.500 | 3465 |
| $N = 7$ | 1.251 | 5940 | 2.158 | 5940 | 1.745 | 5940 |
| $N = 9$ | 1.325 | 9075 | 2.649 | 9075 | 1.836 | 9075 |
| | | | LE | | | |
| | 1.397 | 10750 | 2.981 | 10560 | 1.919 | 10446 |

Figures 3, 4, and 5 show axial and shear stress components variation span-wise for the three different structural configurations. A simplified analytical solution was considered for the full model (Fig. 2a) of the three-bay wing box for comparison purposes. This analytical solution can be found in the book by Rivello.[2]

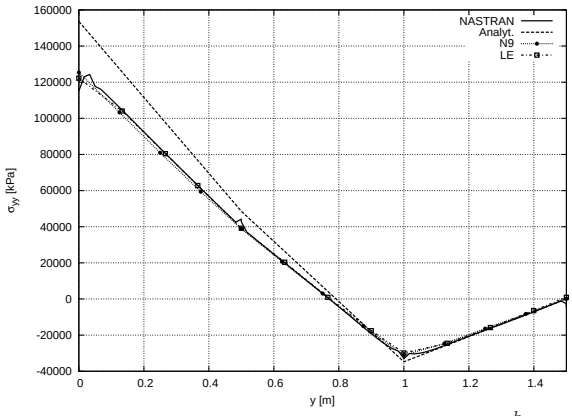


(a) Bottom right spar cap; $\sigma_{yy}$ at $x = b$, $z = -\frac{h_2}{2}$

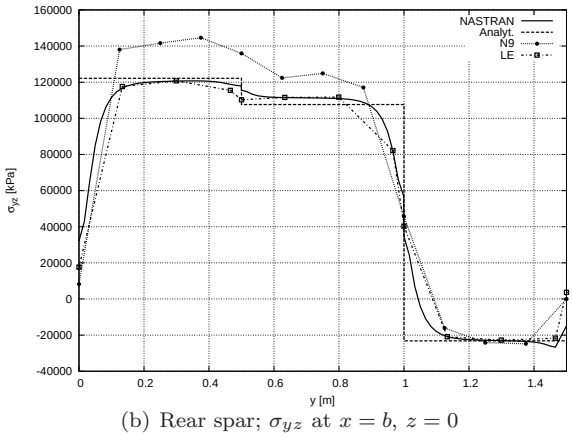


(b) Rear spar; $\sigma_{yz}$ at $x = b$, $z = 0$

**Figure 3. Stress components distribution along the wing span. Comparison of analytical, MSC/NASTRAN© and CUF models, full model (Fig. 2a) of the three-bay wing box.**

Finally, Table 2 reports stress components values of both LE and SOLID/SHELL models. The following remarks can be made.

1. Refined beam theories, especially LE, allows us to obtain the results of the solid model (which is the most accurate and at the same time the most computational expensive).

2. The number of degrees of freedom of the present models is significantly reduced with respect to MSC/NASTRAN© solid model.

3. Both MSC/NASTRAN© and higher-order CUF models, unlike analytical theories based on idealized stiffened-shell structures and classical 1D models, allow to make evident the effects due to ribs and open sections.

4. The Component-Wise capability of the present LE approach is clearly evident from the conducted analysis.

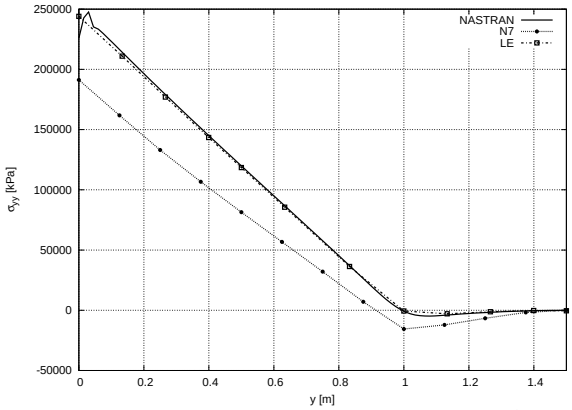


(a) Bottom right spar cap; $\sigma_{yy}$ at $x = b$, $z = -\frac{h_2}{2}$

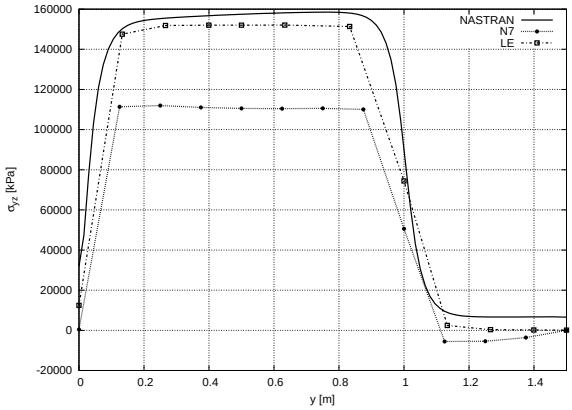


(b) Rear spar; $\sigma_{yz}$ at $x = b$, $z = 0$

**Figure 4. Stress components distribution along the wing span. Comparison of MSC/NASTRAN© and CUF models, three-bay wing box with no ribs (Fig. 2b).**

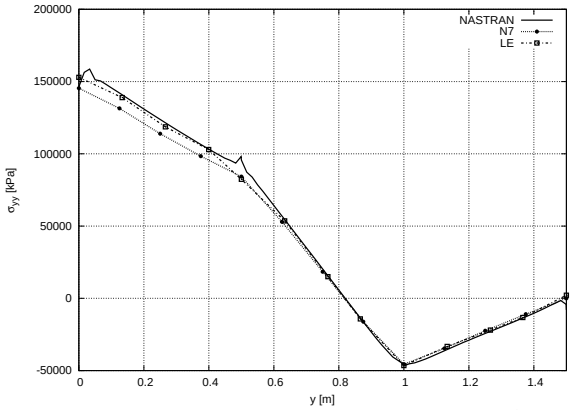


(a) Bottom right spar cap; $\sigma_{yy}$ at $x = b$, $z = -\frac{h_2}{2}$

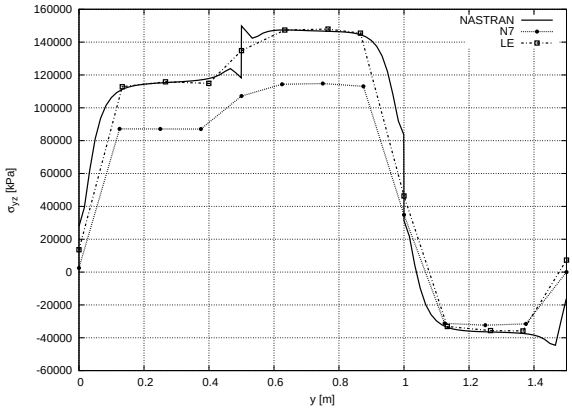


(b) Rear spar; $\sigma_{yz}$ at $x = b$, $z = 0$

**Figure 5. Stress components distribution along the wing span. Comparison of MSC/NASTRAN© and CUF models, three-bay wing box with the open mid-bay (Fig. 2c).**

**Table 2. Stress components, $\sigma_{yy}$ at $[b, \frac{l}{2}, -\frac{h_2}{2}]$ and $\sigma_{yz}$ at $[b, \frac{l}{2}, 0]$, of the three-bay wing box.**

| | Case 1, fig. 2a | | Case 2, fig. 2b | | Case 3, fig. 2c | |
|---|---|---|---|---|---|---|
| Model | $\sigma_{yy}$ [MPa] | $\sigma_{yz}$ [MPa] | $\sigma_{yy}$ [MPa] | $\sigma_{yz}$ [MPa] | $\sigma_{yy}$ [MPa] | $\sigma_{yz}$ [Pa] |
| MSC/NASTRAN© | 80.598 | 120.730 | 178.147 | 155.368 | 123.841 | 115.351 |
| LE | 80.404 | 120.603 | 177.018 | 151.876 | 118.684 | 115.810 |

### III.B. Free Vibration Analysis of a Thin-walled Cylinder

The modal analysis of a typical fuselage structure was carried out. The cross-section of the structure is shown in Fig. 6.

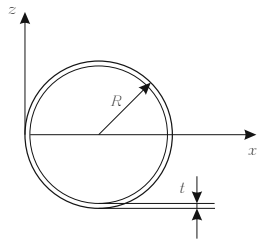


**Figure 6. Thin-walled cylinder.**

The longitudinal length, $L$, is equal to 15 $[m]$, whereas the radius, $R$, of the circular cross-section is 1 $[m]$. The thickness of the thin-walled cylinder is $t = 2 \times 10^{-3}$ $[m]$. A clamp constraint is applied in both of the end of the structure.

**Table 3. Flexural and torsional frequencies of the skin. Comparison between different models.**

| | Frequencies $[Hz]$ | | | | | | |
|---|---|---|---|---|---|---|---|
| | $N=1$ | $N=2$ | $N=3$ | $N=4$ | $N=5$ | $N=6$ | MSC/NASTRAN© |
| $DOFs$ | 306 | 612 | 1020 | 1530 | 2142 | 2856 | 7800 |
| $F$ | 50.656 | 51.458 | 46.590 | 46.531 | 46.510 | 46.499 | 46.951 |
| | 121.945 | 123.345 | 106.500 | 106.266 | 106.093 | 106.015 | 107.640 |
| | 209.589 | 211.282 | 177.589 | 176.826 | 176.696 | 176.675 | 179.360 |
| $T$ | 105.874 | 105.874 | 105.874 | 105.874 | 105.873 | 105.873 | 108.590 |
| | 211.747 | 211.748 | 211.747 | 211.747 | 211.747 | 211.747 | 211.672 |
| | 317.621 | 317.621 | 317.621 | 317.621 | * | * | 317.102 |

* results not found in the first 60 frequencies.

Table 3 quotes the frequencies of the first three flexural ($F$) and torsional ($T$) modes. Column $2^{nd}$ to $7^{th}$ report the results by the TE models. The CUF models were compared with an MSC/NASTRAN© model built with shell finite elements. It must be highlighted that refining 1D CUF models (i.e. increasing the order of the expansion of the cross-section's displacement field) the frequencies converge to smaller values in agreement with the commercial code. Figures 7 and 8 show the first three flexural and torsional modal shapes, respectively.

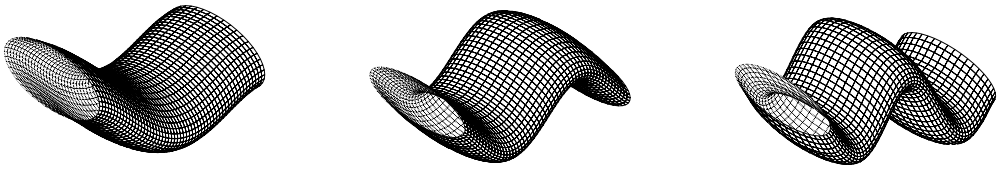

(a) $f = 46.590$ $Hz$ (b) $f = 106.500$ $Hz$ (c) $f = 177.589$ $Hz$

**Figure 7. Flexural normal modes of the thin-walled cylinder. Cubic TE model.**

*Shell–like* modes were detected using the TE higher-order models. These modes are modal shapes that involve wide cross-sectional deformations. The term "shell" is used to denote the fact that these type of modal shapes are usually detectable using plate/shell finite elements. The frequencies of the *shell–like* modes are reported in Table 4. $L$ and $M$ stand for the number of waves that can be identified in the

**Table 4. *Shell–like* mode frequencies. Comparison between different models.**

| Frequencies $[Hz]$ | | | | | | |
|---|---|---|---|---|---|---|
| | | $N=3$ | $N=4$ | $N=5$ | $N=6$ | MSC/NASTRAN© |
| $DOFs$ | | 1020 | 1530 | 2142 | 2856 | 7800 |
| $L=1$ | $M=2$ | 44.435 | 17.578 | 17.510 | 17.495 | 17.579 |
| | $M=3$ | * | 52.871 | 10.534 | 9.808 | 9.409 |
| | $M=4$ | * | * | 58.999 | 12.820 | 8.961 |
| | $M=5$ | * | * | * | 64.023 | 12.450 |
| $L=2$ | $M=2$ | 97.414 | 44.987 | 44.905 | 44.889 | 45.244 |
| | $M=3$ | * | 107.783 | 23.318 | 22.692 | 23.248 |
| | $M=4$ | * | * | 117.294 | 18.115 | 15.473 |
| | $M=5$ | * | * | * | 124.369 | 14.973 |
| $L=3$ | $M=2$ | 161.967 | 81.700 | 81.496 | 81.429 | 82.293 |
| | $M=3$ | * | 167.330 | 44.599 | 44.141 | 43.479 |
| | $M=4$ | * | * | 177.995 | 29.730 | 27.082 |
| | $M=5$ | * | * | * | 186.547 | 21.028 |
| $L=4$ | $M=2$ | 237.043 | 124.579 | 124.061 | 123.964 | 125.470 |
| | $M=3$ | * | 232.448 | 55.574 | 49.808 | 68.681 |
| | $M=4$ | * | * | 241.501 | 45.836 | 42.633 |
| $L=5$ | $M=2$ | 320.597 | 171.417 | 170.252 | 170.098 | 172.290 |
| | $M=3$ | * | 303.373 | 90.234 | 89.992 | 97.712 |
| | $M=4$ | * | * | * | 68.892 | 61.385 |
| $L=6$ | $M=2$ | 410.699 | 220.504 | 218.278 | 217.973 | 217.228 |
| | $M=3$ | * | 379.851 | 120.979 | 120.205 | 127.582 |
| | $M=4$ | * | * | * | 97.772 | 81.577 |
| $L=7$ | $M=2$ | 505.844 | 306.466 | 266.254 | 266.063 | 264.763 |
| | $M=3$ | * | 461.402 | 153.430 | 151.297 | 160.632 |
| | $M=4$ | * | * | * | 136.764 | 104.651 |

* results not found in the first 60 frequencies.

longitudinal direction and cross-sectional direction, respectively. The first *shell–like* mode was correctly detected by the cubic ($N=3$) TE model at least. Increasing the order of the interpolating TE polynomials, the theory becomes able to identify a larger number of modal shapes, while the agreement between the MSC/NASTRAN© model and the TE models is improved. Some *shell–like* modal shapes are depicted in Fig. 9. In conclusion, the analysis of the results suggest the following statements.

1. A linear TE model ($N=1$) is enough to correctly predict the torsional frequencies.
2. Higher than second-order TE models are required to correctly detect the flexural frequencies, in according to MSC/NASTRAN©.
3. At least a cubic-order TE model is necessary to detect the *shell–like* modes. Higher than fourth-order TE models provide a good accuracy, with a considerable low number of the degrees of freedom with respect to MSC/NASTRAN© model.
4. By increasing the number of the expansion terms, the TE models identify even more *shell–like* modes presenting a larger $M$.

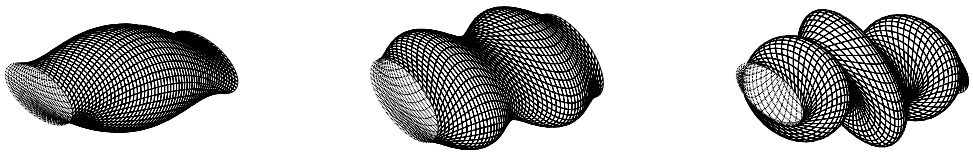

(a) $f = 46.590\ Hz$ (b) $f = 106.500\ Hz$ (c) $f = 177.589\ Hz$

**Figure 8. Torsional normal modes of the thin-walled cylinder. Cubic TE model.**

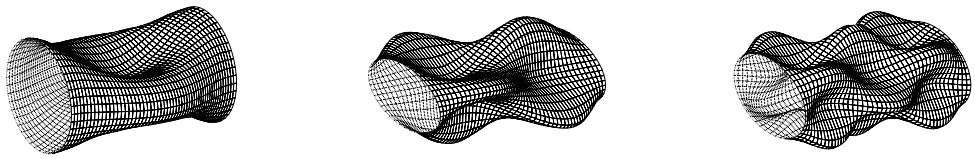

(a) $M = 2$, $L = 1$ (b) $M = 3$, $L = 2$ (c) $M = 4$, $L = 3$

**Figure 9.** $Shell-like$ **modal shapes corresponding to different values of** $M$ **and** $L$**.**

## IV. Conclusions

Two structural problems have been discussed in this paper, including multi-bay box wings and fuselage. Comparisons with solid and shell models from commercial codes were provided. The results obtained suggest the following.

- The proposed refined 1D models offer a good accuracy in detecting the mechanical behavior of aircraft structures. In particular, torsional-bending couples, effects due to ribs and open sections, and shell-like modes are foreseen by opportunely increasing the order of the model.
- The capability offered by the CUF 1D models allows us to deal with a large variety of complex wing structures, such as in Ref. 18, 19, where the LE models are exploited in a CW approach to model a large variety of wing structures.
- The present 1D formulation overcomes the need to combine different structural elements (beam, shell, etc.) to analyze thin-walled structures. In Ref. 22 CUF models have been used for the analysis of complex fuselage configurations, including longitudinal and transversal stiffener members.
- The present formulation is extremely convenient in terms of computational costs if compared to solid models. This aspect is of fundamental importance, since the design of a aircraft involves coupled problems (fluid-structure interaction) and it is often an iterative process.

Further work could be directed to the exploration of more representative examples of aircraft wings and/or fuselages.

## References


[1]Bruhn, E. F., *Analysis and Design of Flight Vehicle Structures*, Tri-State Offset Company, 1973.

[2]Rivello, R. M., *Theory and analysis of flight structures*, McGraw-Hill, 1969.

[3]Vörös, G. M., "A special purpose element for shell-beam systems," *Computers and Structures*, Vol. 29, No. 2, 1988, pp. 301–308.

[4]M.S. Bouabdallah, J. B., "Formulation and evaluation of a finite element model for the linear analysis of stiffened composite cylindrical panels," *Finite Elements in Analysis and Design*, Vol. 21, 1996, pp. 669–682.

[5]Patel, S. N., Datta, P. K., and Seikh, A. H., "Buckling and dynamic instability analysis of stiffened shell panels," *Thin-Walled Structures*, Vol. 44, 2006, pp. 321–333.

[6]Jensen, J. J., "On the shear coefficients in Thimoshenko's beam theory," *Journal of Sound and Vibration*, Vol. 87, 1983, pp. 621–635.

[7]Dinis, P., Camotim, D., and Silvestre, N., "GBT formulation to analyse the buckling behaviour of thin-walled members with arbitrarily branched open cross-sections," *Thin-Walled Structures*, Vol. 44, 2006, pp. 20–38.

[8]Silvestre, N., "Generalised beam theory to analyse the buckling behaviour of circular cylindrical shells and tubes," *Thin-Walled Structures*, Vol. 45, 2007, pp. 185–198.

[9]Carrera, E., Giunta, G., and Petrolo, M., *Beam Structures: Classical and Advanced Theories*, John Wiley & Sons, 2011, DOI: 10.1002/9781119978565.

[10]Reddy, J. N., *Mechanics of laminated composite plates and shells. Theory and Analysis*, CRC Press, 2nd ed., 2004.

[11]Carrera, E., Giunta, G., Nali, P., and Petrolo, M., "Refined beam elements with arbitrary cross-section geometries," *Computers and Structures*, Vol. 88, No. 5–6, 2010, pp. 283–293, DOI: 10.1016/j.compstruc.2009.11.002.

[12]Carrera, E., Giunta, G., and Petrolo, M., *A Modern and Compact Way to Formulate Classical and Advanced Beam Theories*, chap. 4, Saxe-Coburg Publications, Stirlingshire, UK, 2010, pp. 75–112, DOI: 10.4203/csets.25.4.

[13]Carrera, E., Petrolo, M., and Nali, P., "Unified formulation applied to free vibrations finite element analysis of beams with arbitrary section," *Shock and Vibrations*, Vol. 18, No. 3, 2011, pp. 485–502, DOI: 10.3233/SAV-2010-0528.

[14]Carrera, E., Petrolo, M., and Varello, A., "Advanced Beam Formulations for Free Vibration Analysis of Conventional and Joined Wings," *Journal of Aerospace Engineering*, 2011, In Press.

[15]Carrera, E. and Petrolo, M., "On the Effectiveness of Higher-Order Terms in Refined Beam Theories," *Journal of Applied Mechanics*, Vol. 78, No. 3, 2011, DOI: 10.1115/1.4002207.

[16]Carrera, E. and Petrolo, M., "Refined Beam Elements with only Displacement Variables and Plate/Shell Capabilities," *Meccanica*, Vol. 47, No. 3, 2012, pp. 537–556, DOI: 10.1007/s11012-011-9466-5.

[17]Carrera, E. and Petrolo, M., "A beam formulation with shell capabilities," *Proceedings of 51st AIAA/ASME/ASCE/AHS/ASC Structures, Structural Dynamics, and Materials Conference*, Orlando, Florida, USA, April 2010.

[18]Carrera, E., Pagani, A., and Petrolo, M., "Classical, Refined and Component-wise Theories for Static Analysis of Reinforced-Shell Wing Structures," 2012, To be Submitted.

[19]Carrera, E., Pagani, A., and Petrolo, M., "Component-wise Method Applied to Vibration of Wing Structures," 2012, To be Submitted.

[20]Bathe, K. J., *Finite element procedure*, Prentice hall, 1996.

[21]Carrera, E. and Giunta, G., "Refined beam theories based on a unified formulation," *International Journal of Applied Mechanics*, Vol. 2, No. 1, 2010, pp. 117–143, DOI: 10.1142/S1758825110000500.

[22]Carrera, E., Filippi, M., and Zappino, E., "Free Vibration Analysis of Thin-Walled Structures with Longitudinal and Transversal Stiffeners," 2012, To be Submitted.